Geological Quarterly, 2008, **52** (3): 213–224

Palaeomagnetic age of remagnetizations in Silurian dolomites, Rõstla quarry (Central Estonia)

Jüri PLADO, Ulla PREEDEN, Väino PUURA, Lauri J. PESONEN,
Kalle KIRSIMÄE, Tõnu PANI and Tiiu ELBRA

Plado J., Preeden U., Puura V., Pesonen L. J., Kirsimäe K., Pani T. and Elbra T. (2008) — Palaeomagnetic age of remagnetizations in Silurian dolomites, Rõstla quarry (Central Estonia). Geol. Quart., **52** (3): 213–224. Warszawa.

Alternating field and thermal demagnetization of dolomite samples from the Silurian (Llandovery) horizontally-bedded sequence of central Estonia reveal two secondary magnetization components (A and B) both of chemical origin. A low-coercivity (demagnetized at ≤50 mT) component A ($D = 60.7°$, $I = 7.7°$, $\alpha_{95} = 16.6°$) with high dispersion ($k = 14.2$), yields a palaeopole at 18.2°N and 139.5°E that points towards the Late Devonian — Mississipian segment of the Baltica APWP (Apparent Polar Wander Path). A high-coercivity component B ($D = 13.5°$, $I = 60.7°$, $k = 67.0$, $\alpha_{95} = 4.7°$) carries both normal and reversed polarities. Comparing the palaeopole (71.1°N and 173.3°E) with the European APWP reveals a Cretaceous age. These two remagnetizations are linked to mineral assemblages of magnetite and maghemite (A), and hematite (B) determined from mineralogical (X-ray, SEM and optical microscopy) and rock magnetic (acquisition and thermal demagnetization of a 3-component IRM; Lowrie-test) studies. The results suggest that the first (A) Palaeozoic remagnetization was caused by low-temperature hydrothermal circulation due to the influence of the Caledonian (more likely) or Hercynian Orogeny after the diagenetic dolomitization of carbonates. Hematite, carrying the component B, and goethite, are the latest ferromagnetic minerals that have precipitated into the existing pore space (hematite) and walls of microscopic fractures (goethite) that opened to allow access for oxygen-rich fluids during the Late Mesozoic.

Jüri Plado, Ulla Preeden, Väino Puura, Kalle Kirsimäe and Tõnu Pani, Department of Geology, University of Tartu, Vanemuise 46, 51014 Tartu, Estonia; e-mails: juri.plado@ut.ee, vaino.puura@ut.ee, ulla.preeden@ut.ee, kalle.kirsimae@ut.ee, tpani@ut.ee; Lauri J. Pesonen and Tiiu Elbra, Division of Geophysics, Department of Physical Sciences, University of Helsinki, PO Box 64, FIN-00014 Helsinki, Finland; e-mails: lauri.pesonen@helsinki.fi, tiiu.elbra@helsinki.fi *(received: May 14, 2007; accepted: March 11, 2008).*

Key words: Estonia, Baltica, Silurian, palaeomagnetism, remagnetization, dolomites.

INTRODUCTION

We applied rock magnetic and mineralogical methods to specify the age of magnetic minerals in dolostones from the Rõstla quarry (58.7°N, 25.8°E) Central Estonia (Fig. 1A) in order to establish their post-sedimentational history. The exposed thickness of the dolostones, mined for building stone, is about 7 m. Stratigraphically, the dolomites belong to the Mõhküla Beds that form the uppermost part of the Raikküla Stage, dating to the middle Llandovery (443–428 Ma), Early Silurian (Fig. 1B). The beds formed in shoal to open shelf conditions at the end of the differentiation stage (late Caradoc–mid Llandovery) of the Baltic Palaeobasin (Nestor and Einasto, 1997). The skeletal remains of fossils and lithological characteristics support a normal marine origin of primary carbonates. Teedumäe *et al*. (2001), who gave a detailed description of the Rõstla section, noted two dolomitization events associated with the section at Rõstla. According to their interpretation of the X-ray fluorescence and geological data, the first event occurred soon after deposition, probably at the end of the mid Llandovery (Silurian). Later events of mineralization (including dolomitization and karstification) have altered the rocks along fracture and disturbance zones mainly. Jürgenson (1970) suggested that the dolomitization was a long-lasting process, which took place mainly after the Devonian, whereas Vingisaar and Taalmann (1974) proposed a Late Silurian–Early Devonian late diagenetic age for all varieties of Estonian dolomites. Also, a hydrothermal origin of dolomitization has been proposed for the fracture zone-related sulphide-bearing dolomite bodies (Vaher *et al*., 1962).

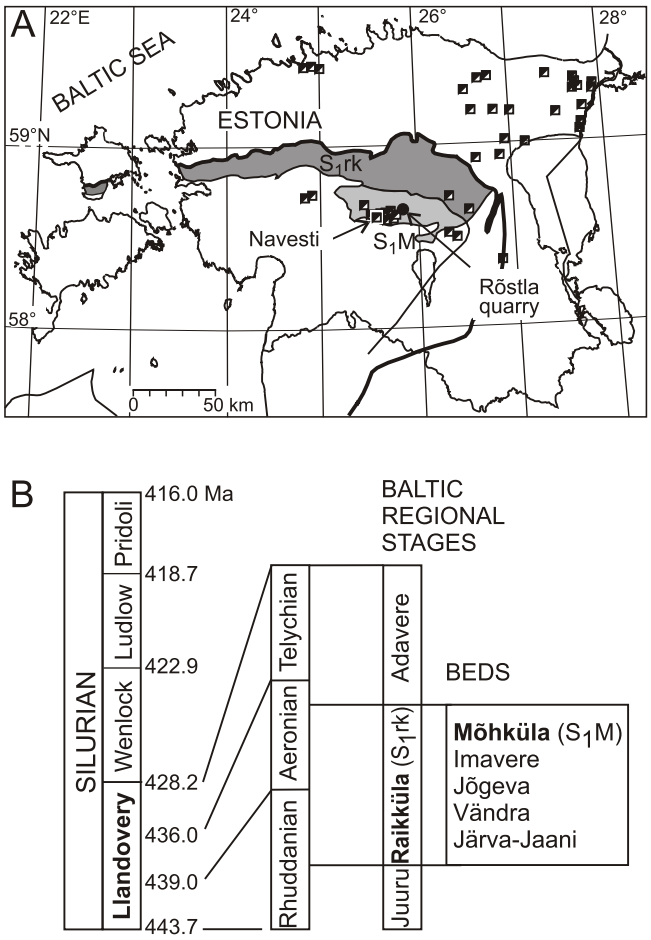

Fig. 1A — outcrop area of the Raikküla Stage (dark grey) and Mõhküla Beds (light grey) in Central and Western Estonia; B — Silurian stratigraphic log indicating the chronostratigraphic position of the Raikküla Stage and Mõhküla Beds

A — thick black line contours approximate distribution of the carbonate rocks of the Raikküla Stage, the thin line contours the distribution of the Mõhküla Beds. The map is redrawn after Nestor (1997). It also locates finds of sulphide mineralization (black-and-white squares) after Bylino *et al.* (1970). **B** — ages are from Gradstein *et al.* (2004)

SAMPLES AND METHODS

Twenty-six hand-samples (RR1–RR9, RS1–RS10, RO1–RO7), which represent three varieties (hereafter I, II and III) of dolomites, were collected from the Rõstla quarry in different years (1998, 2004, 2005) and thus, from different positions of the face. The samples were oriented with a geological compass taking the effect of declination (~5°) into account. Variety I comes from the uppermost interval of the quarry (samples RR1–RR3, RS3, RS4, RS8–RS10, RO3, RO4 and RO10). It represents a finely crystalline, pale yellow dolomite with reddish nodular areas. The nodular areas are coarser and more porous, and have sharply violet-tinged rims at the contacts with the finely crystalline parts (Fig. 2A, B). Variety II, micro- to finely crystalline (Fig. 2C), mainly pale beige, wavy- or nodular-bedded argillaceous dolomite, is represented by samples RR4–RR6, RS1, RS2, RS7, RO1, RO2 and RO6. In places, this variety has a black, red or violet colour within the lense-like interbeds of skeletal-silicified grainstone, or, in nodules. Massive dolomite dyke-like bodies that cross-cut the quarry represent the third variety (samples RR7–RR9, RS5, RS6 and RO5, Fig. 2D). These consist of medium to coarse-grained (locally greenish-grey) dolomites that do not show any sedimentary features but contain relatively voluminous (up to a several hundreds cm^3) caverns. Overall, the walls of caverns show large (up to a few mm) rhombs of dolomite crystals with rare rusty impregnation. Most likely, the third variety of dolomites post-date varieties I and II.

Representative parts of the hand-samples were used for mineralogical and petrophysical (density and porosity) studies at the Department of Geology, University of Tartu; and another part for magnetic studies at the Laboratory for Palaeomagnetism, Geological Survey of Finland and at the Solid Earth Geophysics research laboratory, University of Helsinki, Finland. Thin sections of the samples were studied microscopically. The mineral composition of selected whole-rock samples and mineral fractions were investigated as unoriented powder preparations on a *Dron-3M* diffractometer using Ni-filtered Cu *Kα* radiation from 2 to 55°, 2θ with 0.02° 2θ step size, and 5 s counting time. The quantitative mineral composition of the samples was found by the full-profile Rietveld method by using *Siroquant 2.5*^{TM} code (Taylor, 1991). Scanning electron microscope and electron microprobe studies were performed at the Institute of Electron Optics, Oulu University.

A total of 233 cylindrical specimens were drilled from samples. The densities and porosities of the specimens were determined with the Archimedes principle by weighing the water-saturated and oven-dried specimens in air and water. Measurements of magnetic susceptibility (χ) and natural remanent magnetization (NRM) were made. Most of the specimens were demagnetized stepwise with an alternating field (AF) of up to 160 mT. In several cases the demagnetization was stopped earlier, when the intensity of NRM decreased below the level of instrumental noise (~0.03 mAm^{-1}). After each step the intensity and direction of NRM were measured using a superconducting (SQUID) magnetometer. Eleven specimens were thermally demagnetized until the 680°C or thermal step (usually between 250 to 500°C) when a drastic increase in magnetic susceptibility or remanence occurred, reflecting mineralogical changes due to heating (goethite/maghemite to hematite, see e.g., Dunlop and Özdemir, 1997). Individual NRM measurements were subjected to a joint analysis by stereographic plots, demagnetization decay curves, orthogonal demagnetization diagrams (Zijderveld, 1967), and principal component analysis (Kirschvink, 1980) to obtain the characteristic remanence directions. Fisher (1953) statistics was used to calculate mean remanence directions. To identify the carriers of remanence, eleven samples were tested by coercivity (with a maximum available magnetizing field of 1.5 T) and unblocking temperature properties (Lowrie, 1990; Fig. 3) by step-wise heating in air.

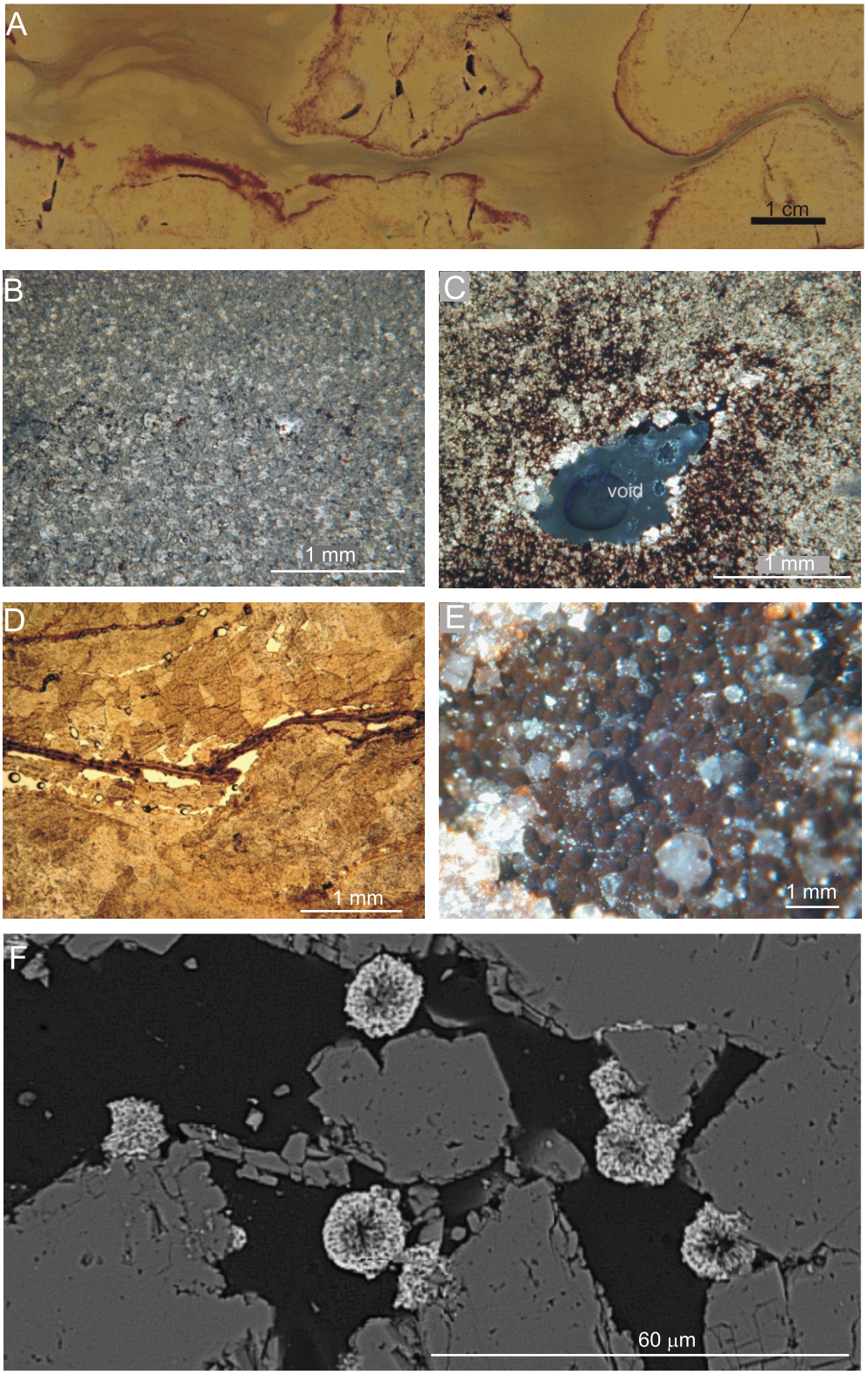

Fig. 2. Macro- and microscopic photos of the Rõstla dolomites

A — finely crystalline yellow dolomite (variety I) with violet hematite-rich concentrations that contain coarser dolomite crystals and is more porous than the surroundings rock; **B** — finely crystalline dolomite in plane polarized light, sample RR1 (variety I). The photograph is taken from the sharp violet-tinged rim representing higher hematite concentrations. Inside the reddish nodule-like hematite-rich masses (the lowermost part of the photo) the dolomite crystals are coarser (0.04–0.15 mm), whereas in the outside part (the uppermost part of the photo) the crystals are finer, with diameters of <0.05 mm; **C** — dolomite (paler) crystals and hematite (darker) surrounding an ~1.5 mm open void (sample RR4; variety II). The concentration of hematite is higher adjacent to the void; **D** — concentration of darker minerals is higher along the cracks (specimen RO5–4, variety III); **E** — spheres of goethite (dark) occurring on the walls of dolomite (pale crystals; sample RR2; variety I); **F** — SEM backscattered image of pale radial aggregates (goethite according to morphological parameters; composed of 81 wt.% of iron oxide according to *Electron Probe Microanalyzer* — EPMA data) filling the cracks (black) in dolomite (dark grey; sample RO3; variety I)

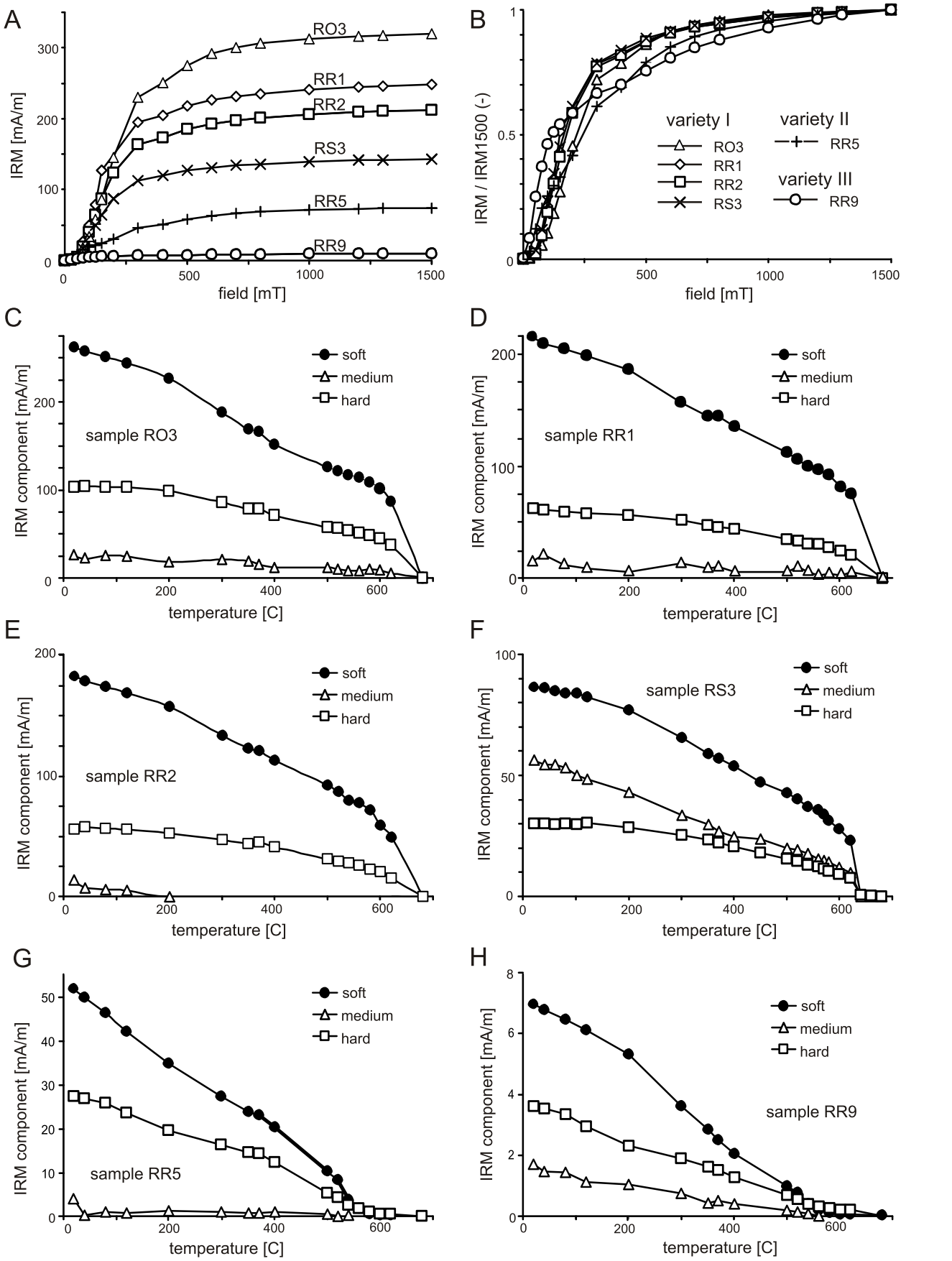

Fig. 3A and B — progressive acquisition of IRM (isothermal remanent magnetization); C–H — thermal demagnetization of a three-component IRM produced by magnetizing the sample in 1500 mT along its *z*-axis, followed by 400 mT along the *y*-axis, and finally 120 mT along the *x*-axis

RESULTS

MINERALOGY

Based on XRD data the samples are dolomites to argillaceous dolomites (Table 1). Most of the samples represent pure dolostones with a dolomite content from 92 to 97%. In three samples of variety II the dolomite content is somewhat lower (71–76%), the rest being clay minerals, quartz and K-feldspar. The only magnetic mineral recognized in whole-rock samples in a detectable amount (i.e. >0.5%) is hematite, which comprises up to 2.2% of the composition of variety II. Binocular microscopic and SEM observations reveal that, apart from hematite, the presence of goethite that occurs as secondary reddish to dark-brown spherolitic aggregates in the form of surface coatings on fracture planes and dissolution mould walls (Fig. 2E, F).

The yellowish and reddish argillaceous finely crystalline dolomite of varieties I and II is composed of micro-to-finely crystalline (<0.05 mm) masses of tightly interlocking anhedral-to-subhedral dolomite crystal mosaics, which may contain floating, medium-crystalline (0.05–0.2 mm) dolomite euhedral rhombs. Dolomite crystals are cloudy and both in plane and polarized light are unzoned. The subhedral crystals have mostly planar boundaries (Fig. 2B)

Varieties I and II contain patches and laminaes of medium-to-coarsely crystalline (0.05–0.5 mm) dolomite porous frameworks, which are frequently found around fractures and (crinoid) dissolution moulds. The intergranular pores of these areas are filled with submicroscopic hematite masses giving a reddish or dark violet colour (Fig. 2A–C). Hematite in reddish-coloured areas and belts of the finely-to-microcrystalline dolomite occurs along the intergranular contacts of the dolomite crystallites and it is preferentially concentrated along the boundaries with the medium-to-coarse dolomite areas (Fig. 2B).

Variety III is composed of replacive medium-to-coarse crystalline (>0.2 mm) anhedral-to-euhedral dolomite rhombs that vary in grain size, and which are remarkably more coarse-grained (up to several mm) towards the abundant fractures and cavities. The crystals are turbid and commonly complexly zoned in plane polarized light. The crystal boundaries of the euhedral dolomite crystallites are mainly nonplanar (tangential) and crystal boundaries are rarely partly curved. The euhedral dolomite individual crystals are in most cases cemented by intergranular xenomorphic dolomite, which shows sector-like extinctionin polarized light.

The acquisition curves of isothermal remanent magnetization (IRM; Fig. 3A, B) reveal steep (at <0.3 to 0.4 T) and gentle (at >0.3 to 0.4 T) gradients with no saturation reached in 1.5 T. Thermal demagnetization curves of the 3 axes IRM from variety I samples (Fig. 3C–F) show a relatively smooth decay at the soft and hard fractions indicating a domination of hematite at a wide range of coercivities. The demagnetization curve of the medium (0.12 to 0.4 T) fraction shows, additionally to the signal by hematite (Fig. 3C, F), slightly steeper gradients between 350 to 400°C (Fig. 3C, F) and 520 to 560°C indicating the presence of some maghemite and magnetite. Signal of hematite at the low-coercivity fraction curves may be due to the presence of large multi-domain grains or indicates heat-caused mineralogical changes during the treatment. Varieties II and III reveal hematite producing the high (0.4 to 1.5 T) coercivity component (Fig. 3G, H) whereas magnetite and possibly some maghemite (Fig. 3H) are responsible for the demagnetizing behaviour of the soft and medium coercivity fractions. No clear

Table 1

Quantitative mineral composition of Rõstla dolomites by XRD powder patterns

Specimen	PS	Chlorite	Illite	Quartz	K-feldspar	Albite	Dolomite	Hematite
variety I								
RR1-3c	$A+B_N$	–	2.4 ±0.8	1.5 ±0.2	2.3 ±0.5	2.1 ±0.4	91.7 ±1.0	tr
RR2-1c	$A+B_N$	–	2.7 ±0.8	1.9 ±0.2	2.9 ±0.5	tr	92.5 ±0.9	–
RR3-1c	$A+B_N$	–	1.4 ±0.6	1.1 ±0.1	1.4 ±0.3	0.7 ±0.3	95.4 ±0.7	–
variety II								
RR4-1d	$A+B_R$	2.7 ±0.4	7.9 ±0.6	8.1 ±0.1	8.5 ±0.3	–	70.6 ±0.6	2.2 ±0.1
RR5-3d	$A+B_N$	2.5 ±0.4	6.1 ±0.6	6.7 ±0.1	8.1 ±0.4	–	75.4 ±0.6	1.2 ±0.1
RR6-1f	A	1.9 ±0.4	6.2 ±0.6	6.2 ±0.1	8.6 ±0.4	–	76.0 ±0.6	1.1 ±0.1
RS1-3a	$A+B_N$	–	tr	1.6 ±0.2	1.9 ±0.3	1.4 ±0.3	94.3 ±0.5	tr
RS2-3d	–	–	tr	1.8 ±0.2	1.1 ±0.5	0.6 ±0.5	96.5 ±0.7	tr
variety III								
RR7-6c	–	–	2.8 ±0.7	1.0 ±0.2	1.6 ±0.4	1.4 ±0.4	93.2 ±0.8	–
RR8-3c	–	–	3.8 ±0.6	1.4 ±0.1	1.7 ±0.3	1.2 ±0.3	91.9 ±0.7	–
RR9-3c	–	–	2.8 ±1.2	1.2 ±0.2	1.0 ±0.7	tr	94.4 ±1.4	–

PS — palaeomagnetic signature (see text and Table 3 for explanations), where A (B) denotes presence of two different remanence directions. Subindex N(R) denotes normal (reversed) polarity of the characteristic remanence; tr — traces of mineral observed

indications of goethite, which has been found by mineralogical studies, have been found during the IRM test. It's possible that goethite has not been saturated due to the relatively low field used to magnetize the samples, or is non-magnetic.

PHYSICAL PROPERTIES

The grain densities of the Rõstla dolomites (Table 2) are lower than that of theoretical dolomite (2866 kg m^{-3}; e.g., Johnson and Olhoeft, 1984) and the contrasts between different varieties are negligible. Varieties I and II have high porosities (Table 2 and Fig. 4), which are most likely due to volume reduction by replacement of original carbonates (mainly calcite) by dolomite, as the latter has a smaller molar volume. Variety III has relatively low differences between grain and wet densities as mirrored in their low porosity (Table 2). However, due to the relatively small sizes of specimens (~11 cm^3), the effect of macro-porosity is not, taken into account thus the overall po-

Table 2

Physical properties of dolomites from the Rõstla quarry

Var.	PS	N_S	ρ_G [kg m^{-3}]	ρ_W [kg m^{-3}]	ϕ [%]	χ [10^{-6} SI]	NRM [mA m^{-1}]	Q [–]
I	A+B	11	2801 ±16	2596 43	11.4 2.7	8 2	0.78 0.46	4.6 3.8
II	A+B	9	2800 ±15	2635 77	9.2 3.6	18 12	0.28 0.41	0.4 0.3
III	–	6	2806 ±38	2740 65	3.7 1.7	15 7	0.07 0.03	0.2 0.2
Total		26	2802 22	2643 ±83	8.9 4.1	13 9	0.44 0.48	2.1 3.2

Var. — variety of sampled dolomites (see text for I, II, and III), PS — palaeomagnetic signature, where A, B denotes presence of two different remanence directions, N_S — number of samples, $_G$ — grain density, $_W$ — wet density, — porosity, — magnetic susceptibility (volume normalized), NRM — intensity of the natural remanent magnetization, Q — Koenigsberger ratio

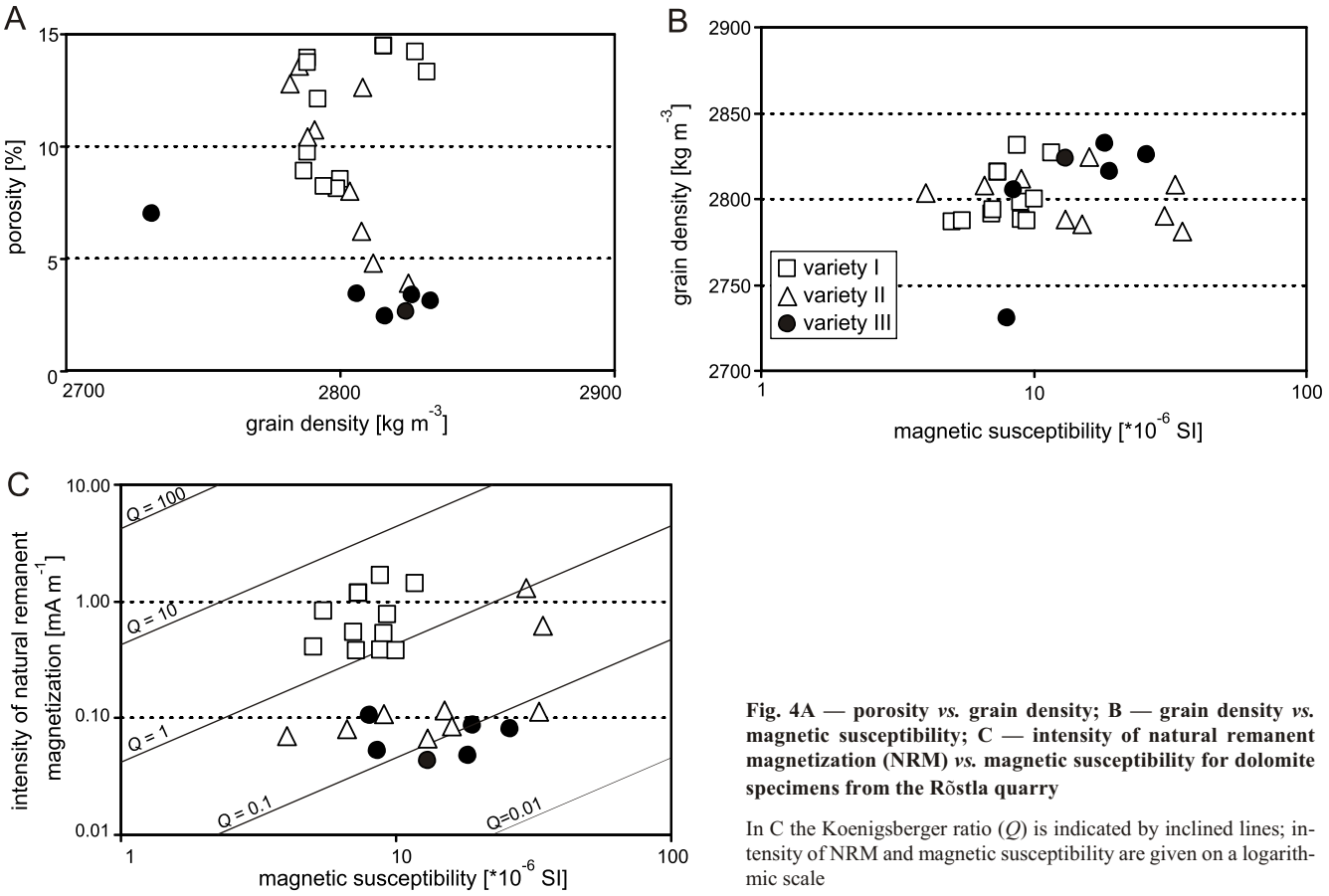

Fig. 4A — porosity *vs.* grain density; B — grain density *vs.* magnetic susceptibility; C — intensity of natural remanent magnetization (NRM) *vs.* magnetic susceptibility for dolomite specimens from the Rõstla quarry

In C the Koenigsberger ratio (Q) is indicated by inclined lines; intensity of NRM and magnetic susceptibility are given on a logarithmic scale

rosity of the variety III type of dolomites is higher than the laboratory porosity due to the presence of visible vugs, which are comparable to the sizes of the specimens.

Based on the values of natural remanent magnetization intensity, the samples are divided into two groups with relatively high and low values of NRM. The first group, represented by the first variety of dolomites, reveals high intensities (NRM >0.4 mA m^{-1}). The ferruginous-rich specimens of variety II belong to this group as well (Fig. 4C). The second group, with much lower intensity (NRM <0.4 mA m^{-1}), is represented by variety III (Table 2) and the light-coloured (non-ferruginous) specimens of the second variety belong also to group 2. Because of the high internal mineralogical and magnetic inhomogeneity of variety II the standard deviation of NRM intensities is large (Table 2). The two groups can be differentiated also by their Koenigsberger ratios (group 1: $Q > 0.5$; group 2: $Q < 0.5$). The discrepancies in Q are mainly in the variation in NRM, since the magnetic susceptibilities (Fig. 4B, C) are uniform and relatively low (<100 × 10^{-6} SI) in all samples. Slightly higher susceptibility values were measured for variety II; however, these values correlate neither with NRM intensity data nor with the intensity of impregnation.

PALAEOMAGNETIC BEHAVIOUR

Two remanent magnetization components (hereafter called A and B) were identified by directional groupings, alternating field (AF) coercivity and thermal spectra (Figs. 3 and 5). Both components are present in varieties I and II with NRM intensities generally >0.2 mA m^{-1}. Variety III has extremely weak NRM (Table 2) generally without detectable remanent magnetization components. The two components differ in their stability against the AF demagnetization: component A is softer and removed at fields ≤50 mT whereas component B is more resistant to AF, as in many specimens it has not yet been totally removed at 160 mT, the maximum field applied (Fig. 5). Specimens with higher resistance against the AF course (e.g., Fig. 5B, D, E) usually exhibit both components of remanence, whereas specimens with lower resistance (Fig. 5A and C) show up component A only, if at all. Both polarities are present in component B with antipodal symmetry B_N (Fig. 5B and G) and B_R (Fig. 5E and F), and they pass the reversal test (category B; McFadden and McElhinney, 1990). During the course of thermal demagnetization the low coercivity (A) component is observable until 200 to 320°C, being partly overshadowed by temperature-caused changes in carriers of remanence. The pale samples without visible hematite concentrations tend to reveal component A only (e.g., Fig. 5H). The majority of the thermally demagnetized specimens show an abrupt increase in magnetic susceptibility and/or intensity of the NRM at between 300 and 400°C, indicating mineralogical changes. Comparing the demagnetization results with the magnetic mineralogy (Fig. 2), and coercivity spectra (Fig. 3), we suggest that component A is carried by magnetite, maghemite and possibly some large multidomain hematite, whereas hematite is responsible for component B.

The combined sample-mean direction of B (Table 3) is slightly shifted from the present Earth's magnetic field (PEF) at the Rõstla site ($D \approx 6°$, $I \approx 72°$). However, the component's unlikely to represent viscous remanent magnetization (VRM) as it does not demagnetize at elevated temperatures. Also, the presence of the reversed counterpart does not support its viscous origin. We suggest B represents a magnetic overprint that, carried by hematite, is chemical in origin.

The low-coercivity component A1, of single polarity, has a mean direction (Table 3) that is clearly different from PEF and B. To avoid the effect of possible overlap between the coercivities of A and B, and to get more reliable approximation, we calculated the component A (A2 in Table 3, Figs. 6 and 7) from seven samples that are (i) demagnetized thermally or/and (ii) lacking a significant signal from component B. In spite of the lower number of samples, dispersion is somewhat higher (k = 14.2) as compared with A1. The relatively low precision of component A is mainly caused by variation in declinations, whereas the inclination is more stable (Fig. 6). The shallow inclination of the component A concords with palaeogeographic reconstructions where Baltica occupied low northerly latitudes on its way northwards at Late Devonian to Carboniferous times (e.g., Torsvik, 1998).

DISCUSSION

The uniform very fine-to-fine grain size, unzoned and cloudy petrographic character, the planar crystal contacts of the dolomite crystallites, as the well as preservation of primary sedimentary textures, suggest diagenetic dolomitization of the varieties I and II found at Rõstla. In contrast, the medium-to-coarse crystalline dolomite with abundant nonplanar crystal boundaries and zoned overgrowths in cross-cutting vein-like bodies (variety III) suggests significant recrystallization. The paragenetic relationships of the dolomite with possible magnetic carrier Fe-minerals suggest that the hematite and goethite postdate the diagenetic dolomitization. Hematite impregnates the nodular areas and goethite occurs as secondary coatings on the fracture and mould walls. Hematite seems to be responsible for the remanent magnetization component B. Low- to medium-coercivity ferromagnetic minerals such as magnetite, possibly some maghemite and large multidomain hematite, are the cause of the component A.

To find the possible ages for components A and B, we plotted them (see Table 3) on the Apparent Polar Wander Path (APWP) for Baltica (Fig. 7A) and Europe (Fig. 7B; Besse and Courtillot, 2003). The APWP of Baltica includes poles from stable Europe of Late- and post-Carboniferous times (200–300 Ma; Torsvik *et al*., 2001). It was constructed with the spherical spline method with a smoothing parameter of 200 weighted according to the reliability criteria (Q-factor; Van der Voo, 1990) of the available poles. We used the GMAP programme of Torsvik and Smethurst (http://www.geophysics.ngu.no). The poles with Q-factor of 5, 6, and 7 selected from the database in Torsvik *et al*. (1996, 2001) were used. Comparison of poles A and B of this study with the APWP sug-

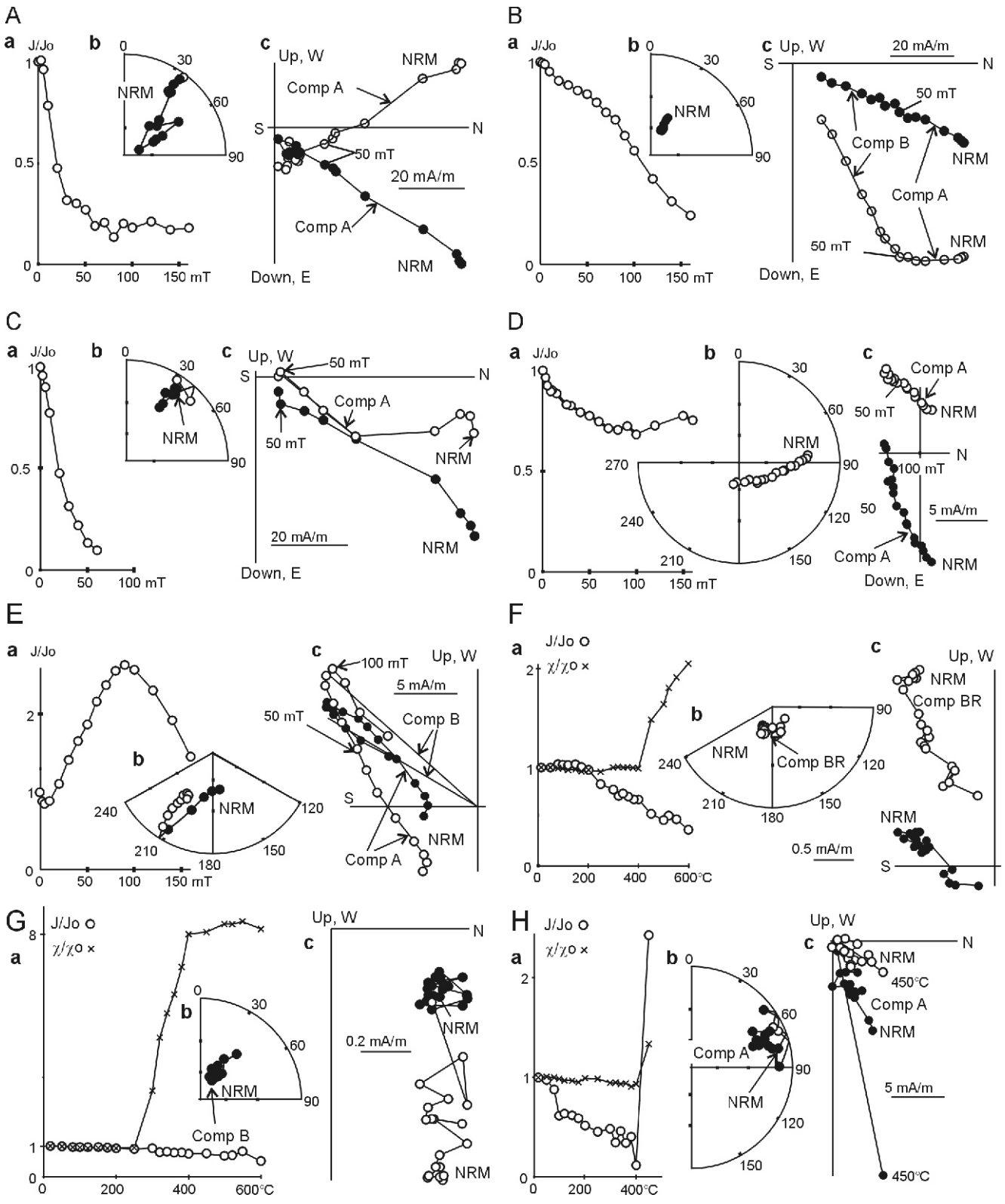

Fig. 5. Examples of alternating field (A–E) and thermal (F–H) demagnetization behaviour characteristic of the Rõstla dolomites

A — specimen RS1-1a; **B** — specimen RS3-1c; **C** — specimen RS7-2a; **D** — specimen RR4-2d; **E** — specimen RO3-2b; **F** — specimen RR4-3b; **G** — specimen RR2-3b; **H** — specimen RR5-1b; **a** — are relative intensity and susceptibility (J/J_0 and χ χ) decay curves, where the demagnetizing alternating field (mT) or temperature (°C) is given on the horizontal axis; **b** — are stereographic projections of directional data on demagnetization; **c** — are the orthogonal demagnetization diagrams, where open (closed) symbols denote the vertical (horizontal planes)

Table 3

Remanence directions and corresponding virtual geomagnetic pole positions calculated as means of samples

Magnetic component	*N* (*n*)	Polarity	*D* [°]	*I* [ ]	*k*	α_{95}	*Plat* [°N]	*Plon* [°E]	*dp* [°]	*dm* [°]
A1	19 (138)	N	47.0	15.4	8.9	11.9	27.9	150.7	6.3	12.2
A2	**7 (27)**	**N**	**60.7**	**7.7**	**14.2**	**16.6**	**18.2**	**139.5**	**8.4**	**16.7**
B_N	11 (68)	N	2.0	63.1	81.4	5.1	75.9	200.0	6.3	8.0
B_R	4 (26)	R	201.0	–53.9	86.3	9.9	62.1	166.7	9.7	13.9
B_{comb}	**15 (94)**	**N+R**	**13.5**	**60.7**	**67.0**	**4.7**	**71.1**	**173.3**	**5.5**	**7.2**
B_N+B_R	2 poles	N+R	–	–	–	–	69.3	176.9		–

N (*n*) — number of samples (specimens) revealing the component, *D* — declination, *I* — inclination, *k* — Fisher's (1953) precision parameter, $_{95}$ — radius of a cone of 95% confidence about the mean; *Plat* and *Plon* — the latitude and longitude of the virtual geomagnetic poles, *dp* and *dm* — semiaxes of an oval of 95% confidence of the pole; see text for description of magnetic components

gests a Late Devonian to Carboniferous age for A, and an Early Cretaceous age for B (Fig. 7). However, both poles plot off the Baltic APWP: because the demagnetization spectra of the two components slightly overlap, the two components may have been separated imperfectly. Therefore, the components, especially the low-coercivity component A, may be contaminated by component B. The more reliable approximation, pole A2 from seven samples only, gives a slightly older age compared to A1 (Fig. 7A). We note that the sample-mean directions are relatively similar in their inclinations but differ in their declinations (Fig. 6). The individual sample-mean A poles align subparallel to the Devonian–Carboniferous section of the APWP-curve suggesting that the A poles may also reflect a considerable time of acquisition. Neither A nor B poles point towards the Silurian, therefore, we deduce that a primary magnetization of Silurian age is lost and overprinted by younger events. Both remanence components are likely of chemical origin. Consequently, the diagenetic dolomitization, which

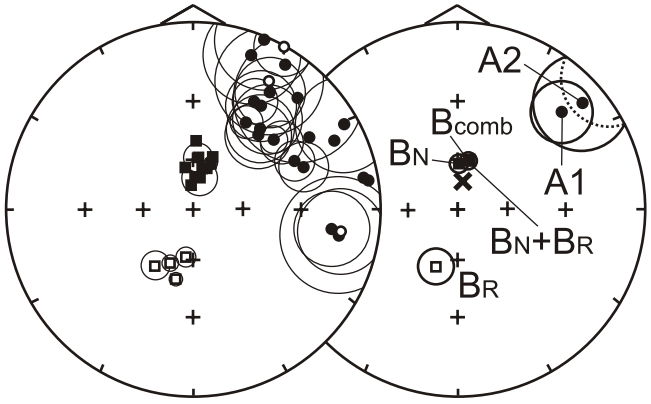

Fig. 6. Equal-angle stereonet projections of *in situ* remanence directions (sample means — left) and the site means (right)

Dots and squares represent components A and B (for data see text and Table 3), respectively. Open (closed) symbols denote upwards (downward) pointing remanence. The circles denote the 95% confidences. Direction of the present Earth field is shown by cross; for other explanations see the text

paragenetically predates the hematite precipitation, must have taken place before the acquisition of component B.

The palaeomagnetic signatures do not assess directly the age of the late replacive dolomitization event carried by variety III dolomites that have completely replaced the earlier carbonates. In a regional context, the exposure of the Mõhküla Beds is located within a NE–SW-trending belt of faults, which often carry dolomitization and Pb–Zn mineralization in Ordovician to Lower Silurian limestones (Puura and Sudov, 1976). In a local view, the Rõstla quarry is situated next to an area with sparse sulphide mineralization (galena, sphalerite, pyrite; see, e.g. Sundblad *et al*., 1999). About 15 km SWW from Rõstla (Fig. 1A) in the excavated trench for the Navesti River, the sulphide mineralization fills large caverns, pores and fissures of the Mõhküla Beds (unpublished observations by Väino Puura in late 1950's). At the Navesti location, thin sulphide and carbonate veins were observed to penetrate the overlying Devonian marlstones, suggesting a post-Devonian age for their formation. Also, the a post-Devonian formation is supported by the fact that the sulphides lack signs of weathering in spite of continental conditions in the Late Silurian (Nestor, 1997) and Early Devonian (Kleesment and Mark-Kurik, 1997) stages.

At Rõstla, the variety III dolomites are spatially related to the numerous fractures and caverns as well as to rare old karst caves and channels 10–30 cm in diameter, suggesting intensive reworking by rock-water interaction. Although sulphide mineralization at the Rõstla quarry is poorly represented, we suggest that the late replacive diagenetic or low-temperature hydrothermal dolomitization is of the same age as in the Võhma–Navesti area. The complexly zoned crystals with a smaller number of unzoned crystals indicate multiple episodes of replacement, overgrowth and also nucleation, which suggest a longer period of activity of these zones rather than a short single impulse of alteration. The formation of low-coercivity ferromagnetic minerals at Rõstla could be related to this interval. Low-temperature orogenically-derived fluid flows are linked in several studies worldwide, e.g. Permian widespread secondary magnetization in North American carbonate and clastic deposits (McCabe and Elmore, 1989) and Tertiary magnetism of the Middle De-

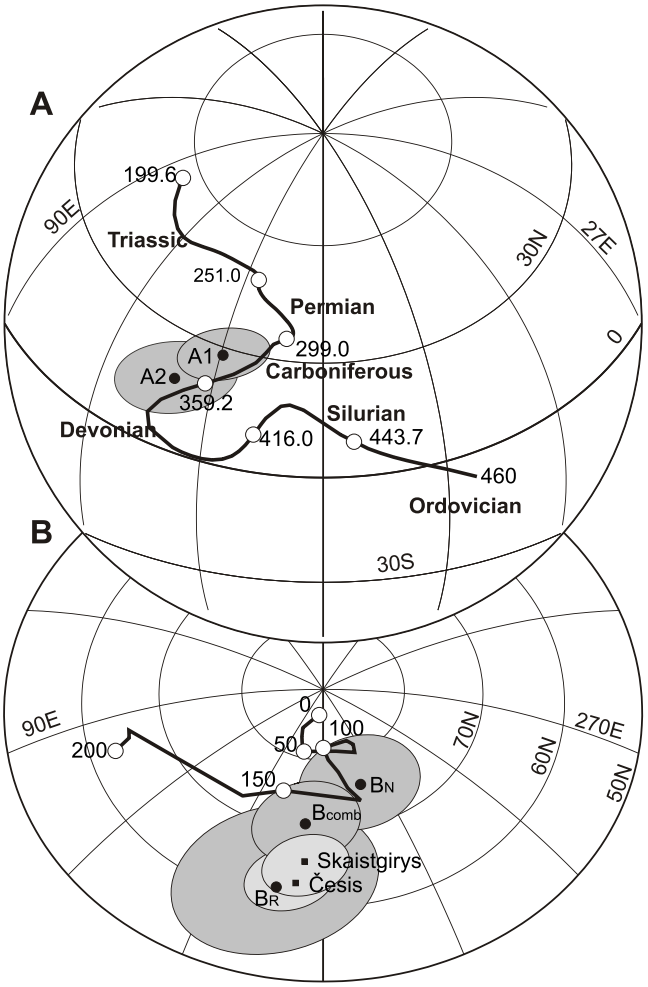

Fig. 7A — combination of (i) APWP path for Baltica (a dark line with white dots of ages in Ma) constructed with the spherical spline method (smoothing parameter = 200; poles with 5 Q 7) weighted according to their *Q*-factor by the GMAP programme of Torsvik and Smethurst (http://www.geophysics.ngu.no), and (ii) two interpretations of pole A (A1 and A2) of the present study (black dots); B — combination of (i) master APW path for Europe for the past 200 Ma (for details see Besse and Courtillot, 2003), (ii) pole B of the present study (black dots), and (iii) poles (black squares) by Katinas and Nawrocki (2004)

The α_{95} confidence circles are given by grey ovals; see text for explanations and interpretations

vonian carbonates of the western Canada Sedimentary Basin (Lewchuk *et al*., 2000).

Our results fit into the following scheme of geological evolution in Central Estonia. Mid Llandovery: deposition of almost pure bioclastic limestones in a shallow NE part of the Ordovician–Silurian Baltic Basin (Nestor and Einasto, 1997), followed by diagenetic dolomitization of limestones in some parts of the basin (Kiipli, 1983). Middle Llandovery to Ludlow: burial of the Mõhküla Beds under a pile of carbonate rocks. It is likely that the primary iron oxides were sulphurated due to anoxic conditions during the diagenesis and burial. Late Silurian to Early Devonian: a far-field expression of the compression by Caledonian tectonics; formation of systems of mainly NE–SW-oriented faults plus erosion and weathering of the overlying Silurian deposits; the Raikküla (including the Rõstla) deposits became exposed (Puura *et al*., 1999). At Rõstla, systems controlling the youngest dolomite bodies as well as karst caves and channels (in which later superposed dolomite mineralization has developed) probably belong to this age. Mid to Late Devonian: burial of the eroded very slightly southerly sloping surface (Puura *et al*., 1999) under transgressive Devonian deposits some hundreds of metres thick. A predominantly continental setting lasted from the Carboniferous to the Paleogene. Puura and Sudov (1976) supposed that lead and zinc sulphide mineralization in association with barite and carbonates in NE and Central Estonia formed due to a post-Devonian regional hydrothermal event. The present study dates the formation of iron oxides (likely due to oxidation of diagenetic sulphides) to the Late Devonian–Carboniferous. Possibly, the brines were slightly heated by Mid to Late Devonian burial causing hydrothermal circulation of fluids and redox gradiends. The event could be tied to the far-field hydrothermal influence of the Caledonian and serve as a source for secondary dolomitization and variety III dolomites. Caledonian induced mobilization of several elements in the Precambrian crust of the Fennoscandian Shield has been observed and dated to 450 Ma (U–Pb, Vaasjoki *et al*., 2002) and ~400 Ma (Sm–Nd age of fluorite, Alm *et al*., 2005). Our study cannot exclude the possible influence of Hercynian tectonism that is somewhat more coeval with the Late Devonian–Carboniferous age of component A. Hercynian tectonism has been associated with simultaneous block tectonics and mafic intrusions in NE Poland (Krzemińska *et al.*, 2006) and the southern part of the Baltic seabed (Puura *et al*., 1991).

During the following predominantly continental and oxygen-rich humid interval, hematite, which post-dates the dolomites according to the present study, was precipitated into the pore space of variety I and II dolomites predominantly. Results similar to our hematite-carried component B, have been reported from Upper Devonian dolomites from Latvia (Česis quarry) and Lithuania (Skaistgirys quarry) (Fig. 7). The authors (Katinas and Nawrocki, 2004) have tied the component to chemical remagnetization due to migration of oxidizing fluids at faults that were reactivated during the Late Jurassic–Early Cretaceous. We also note that the area was subjected to a prolonged period of erosion during the Mesozoic and Cenozoic, allowing oxidizing fluids to penetrate deeper and deeper through time even without any specific tectonic events. Variety III dolomites lack the magnetic signal of hematite suggesting that the intergranular porosity of these dolomites was too low for fluid flow (see Table 2) and, precipitation of secondary hematite. During the Neogene continental period, the Raikküla and Mõhküla deposits became exposed and, finally, buried under a thin cover of Quaternary deposits.

CONCLUSIONS

Two components of remanent magnetization have been identified in the dolomites of the Mõhküla Beds in the Rõstla quarry by alternating field and thermal demagnetization. A northeasterly-directed component (A) with low inclination

dates to the end of Palaeozoic, presumably Late Devonian to Mississipian, whereas another much steeper component (B) is younger, Cretaceous. There is no indication of any primary Silurian magnetization directions. Mineralogical studies revealed hematite responsible for the high-coercivity component (B). The co-presence of magnetite and possibly some maghemite (component A) has been shown by magnetic tests.

We interpret the first (A) Palaeozoic remagnetization epoch as being caused by low-temperature hydrothermal circulation due to the influence of the Caledonian/Hercynian orogeny taking place after the early diagenetic dolomitization of carbonates but serving as a possible source for secondary dolomitization. Hematite and goethite are the latest ferromagnetic minerals that have precipitated into the existing pore space (hematite) and walls of microscopic fractures (goethite) that opened to allow access for for oxygen-rich fluids during the Late Mesozoic.

Acknowledgements. We are thankful to Dr. S. Mertanen and M. Leino for their permission to use the equipments at the Laboratory for Palaeomagnetism, Geological Survey of Finland. We thank Drs. J. Grabowski, R. Szaniawski, J. Mansfeld and an anonymous reviewer for their comments on the manuscript. The Estonian Science Foundation (grants # 5500, #5817 and # 6613) supported the study.

REFERENCES

ALM E., HUHMA H. and SUNDBLAD H. (2005) — Preliminary Palaeozoic Sm–Nd ages of fluorite–calcite–galena veins in the southeastern part of the Fennoscandian Shield. Swedish Nuclear Fuel and Waste Management Co, Report R-04-27: 1–32.

BESSE J. and COURTILLOT V. (2003) — Correction to "Apparent and true polar wander and the geometry of the geomagnetic field over the last 200 Myr". J. Geophys. Res., **108**: EPM 3 (1–2).

BYLINO L. V., MAKAROV V. G., BORDON I. P., ZARZHITSKIJ G. F., BORDON V. E., KRIVODUBSKAYA Z. V., PUURA V. A., FEDORENKO YA. D., MENAKER E. A. and VASIL'EV B. A. (1970) — Perspectives of search for ore deposits in Bielorussia and Baltic states (in Russian). Sovet. Geol., **13**: 3–14.

DUNLOP D. J. and ÖZDEMIR Ö. (1997) — Rock Magnetism. Cambridge Univ. Press. Cambridge.

FISHER R. (1953) — Dispersion on a sphere. Proc.. Royal Soc., London, **A217**: 293–305.

GRADSTEIN F. M., OGG J. G., SMITH A. G., AGTERBERG F. P., BLEEKER W., COOPER R. A., DAVYDOV V., GIBBARD P., HINNOV L. A., HOUSE M. R., LOURENS L., LUTERBACHER H. P., MCARTHUR J., MELCHIN M. J., ROBB L. J., SHERGOLD J., VILLENEUVE M., WARDLAW B. R., ALI J., BRINKHUIS H., HILGEN F. J., HOOKER J., HOWARTH R. J., KNOLL A. H., LASKAR J., MONECHI S., PLUMB K. A., POWELL J., RAFFI I., RÖHL U., SADLER P., SANFILIPPO A., SCHMITZ B., SHACKLETON N. J., SHIELDS G. A., STRAUSS H., VAN DAM J., VAN KOLFSCHOTEN T., VEIZER J. and WILSON D. (2004) — A Geologic Time Scale 2004. Cambridge Univ. Press. Cambridge.

JOHNSON G. R. and OLHOEFT G. R. (1984) — Density of rocks and minerals. In: Handbook of Physical Properties of Rocks, vol. III (ed. R. S. Carmichael): 1–38. CRC Press. Boca Raton.

JÜRGENSON E. (1970) — Secondary changes of the Silurian sequence (in Russian). In: Silurian of Estonia (ed. D. Kaljo): 96–101. Valgus. Tallinn.

KATINAS V. and NAWROCKI J. (2004) — Mesozoic remagnetization of Upper Devonian carbonates from Česis and Skaistgirys quarries (Baltic states). Geol. Quart., **48** (3): 293–298.

KIIPLI T. (1983) — On the genesis of Ordovician and Silurian dolomites at the contact with Devonian deposits (in Russian). Proc. Estonian Acad. Sc., **32**: 110–117.

KIRSCHVINK J. L. (1980) — The least-squares line and plane and the analysis of palaeomagnetic data. Geophys. J. Royal Astronom. Soc., **62**: 699–718.

KLEESMENT A. and MARK-KURIK E. (1997) — Lower Devonian. In: Geology and Mineral Resources of Estonia (eds. A. Raukas and A. Teedumäe): 107–111. Estonian Acad. Publ., Tallinn.

KRZEMIŃSKA E., WISZNIEWSKA J. and WILLIAMS I. S. (2006) — Early Carboniferous age of the cratonic intrusions in the crystalline basement of NE Poland (in Polish with English summary). Prz. Geol., **54** (9): 1093–1098.

LEWCHUK M. T., AL-AASM I. S., SYMONS D. T. A. and GILLEN K. P. (2000) — Late Laramide dolomite recrystallization of the Husky Rainbow "A" hydrocarbon Devonian reservoir, northwestern Alberta, Canada: paleomagnetic and geochemical evidence. Canadian J. Earth Sc., **37**: 17–29.

LOWRIE W. (1990) — Identification of ferromagnetic minerals in a rock by coercivity and unblocking temperature properties. Geophys. Res. Lett., **17**: 159–162.

MCCABE C. and ELMORE R. D. (1989) — The occurrence and origin of late Paleozoic remagnetization in the sedimentary rocks of North America. Geophysics, **2**: 471–494.

MCFADDEN P. L. and MCELHINNEY M. W. (1990) — Classification of the reversal test in palaeomagnetism. Geophys. J. Internat., **103**: 725–729.

NESTOR H. (1997) — Silurian. In: Geology and Mineral Resources of Estonia (eds. A. Raukas and A. Teedumäe): 89–106. Estonian Acad. Publ., Tallinn.

NESTOR H. and EINASTO R. (1997) — Ordovician and Silurian carbonate sedimentation basin. In: Geology and Mineral Resources of Estonia (eds. A. Raukas and A. Teedumäe): 192–204. Estonian Acad. Publ., Tallinn.

PUURA V. and SUDOV B. (1976) — The tectonically active platform zones on the south slope of the Baltic Shield and their metallogeny (in Russian with English summary). Proc. Acad. Sc. Estonian SSR. Chem. Geol., **25**: 206–214.

PUURA V., AMANTOV A., SVIRIDOV N. and KANEV S. (1991) — Tectonics (in Russian). In: Geology and Geomorphology of the Baltic Sea (ed. A. A. Grigelis): 267–290. Nedra, Leningrad.

PUURA V., VAHER R. and TUULING I. (1999) — Pre-Devonian landscape of the Baltic Oil-Shale Basin, NW of the Russian platform. In: Uplift, Erosion and Stability: Perspectives on Long-term Landscape Development (eds. B. J. Smith *et al*.). Geol. Soc., London,. Spec. Publ., **162**: 75–83.

SUNDBLAD K., KIVISILLA J., PUURA V., JONSSON E. and FEDORENKO J. (1999) — Palaeozoic Pb (±Zn) mineralization in the Baltic Sea region. GFF, **121**: 76–77.

TAYLOR J. C. (1991) — Computer programs for standardless quantitative analysis of minerals using the full powder diffraction profile. Powder diffraction, **6**: 2–9.

TEEDUMÄE A., KALLASTE T. and KIIPLI T. (2001) — Aspects of the dolomitization of the Mõhküla beds (Silurian, Estonia). Proc. Estonian Acad. Sc., **50**: 190–205.

TORSVIK T. H. (1998) — Palaeozoic palaeogeography: a North Atlantic viewpoint. GFF, **120**: 109–118.

TORSVIK T. H., SMETHURST M. A., MEERT J. G., VAN DER VOO R., MCKERROW W. S., BRASIER M. D., STURT B. A. and WALDERHAUG H. J. (1996) — Continental break-up and collision in the Neoproterozoic and Palaeozoic — A tale of Baltica and Laurentia. Earth Sc. Rev., **40**: 229–258.

TORSVIK T. H., VAN DER VOO R., MEERT J. G., MOSAR J. and WALDERHAUG H. J. (2001) — Reconstructions of the continents around the North Atlantic at about the 60th parallel. Earth Planet. Sc. Lett., **187**: 55–69.

VAASJOKI M., APPELQVIST H. J. A. and KINNUNEN K. (2002) — Paleozoic remobilization and enrichment of Proterozoic uranium mineralization in the East Uusimaa area, Finland. In: Lithosphere 2002 Second Symposium on the Structure, Composition and Evolution of the Lithosphere in Finland. Programme and extended abstracts, Espoo, Finland (eds. R. Lahtinen *et al*.). Institute of Seimology, Univ. Helsinki, Report S-42.

VAHER R. M., PUURA V. A. and ERISALU E. K. (1962) — Tectonism of NE Estonia (in Russian). In: Geology of Paleozoic. Valgus, Tallinn.

VAN DER VOO R. (1990) — The reliability of paleomagnetic data. Tectonophysics, **184**: 1–9.

VINGISAAR P. A. and TAALMANN V. A. (1974) — An overview on the dolomitization of lower-Paleozoic carbonate rocks in Estonia (in Russian). Proc. Acad. Sc. Estonian SSR. Chem. Geol., **3**: 237–243.

ZIJDERVELD D. J. (1967) — A.C. demagnetization in rocks: analysis of results. In: Methods in Paleomagnetism (eds. D. W. Collinson *et al*.): 254–286. Elsevier, Amsterdam.